

## Article

# Nongrowing Season CO<sub>2</sub> Emissions Determine the Distinct Carbon Budgets of Two Alpine Wetlands on the Northeastern Qinghai—Tibet Plateau

Chenggang Song<sup>1,2,3,†</sup>, Fanglin Luo<sup>4,5,†</sup>, Lele Zhang<sup>1</sup> , Lubei Yi<sup>6</sup>, Chunyu Wang<sup>4,5</sup>, Yongsheng Yang<sup>4,5</sup>, Jiexia Li<sup>4,5</sup>, Kelong Chen<sup>1,\*</sup>, Wenying Wang<sup>2,5,\*</sup>, Yingnian Li<sup>4,5</sup> and Fawei Zhang<sup>4,5,\*</sup> 

- <sup>1</sup> School of Geographic Sciences, Qinghai Normal University, Xining 810008, China; scg8088@163.com (C.S.); zhang1986lele@163.com (L.Z.)
- <sup>2</sup> School of Life Sciences, Qinghai Normal University, Xining 810008, China
- <sup>3</sup> Qinghai Engineering Consulting Center, Xining 810008, China
- <sup>4</sup> Key Laboratory of Adaptation and Evolution of Plateau Biota, Northwest Institute of Plateau Biology, Chinese Academy of Sciences, Xinning Streets, Xining 810008, China; luofanglin@nwipb.cas.cn (F.L.); wangchunyu@nwipb.cas.cn (C.W.); ysyang@nwipb.cas.cn (Y.Y.); jxli@nwipb.cas.cn (J.L.); ynli@nwipb.cas.cn (Y.L.)
- <sup>5</sup> Institute of Sanjiangyuan National Park, Chinese Academy of Sciences, Xinning Streets, Xining 810008, China
- <sup>6</sup> Forestry Carbon Sequestration Service Center, Qinghai Forestry and Grassland Administration, Xining 810008, China; celtyle@163.com
- \* Correspondence: ckl7813@163.com (K.C.); wangwy0106@163.com (W.W.); fwzhang@nwipb.cas.cn (F.Z.); Tel.: +86-971-6133353 (F.Z.); Fax: +86-971-6143282 (F.Z.)
- † These authors contribute equally.



**Citation:** Song, C.; Luo, F.; Zhang, L.; Yi, L.; Wang, C.; Yang, Y.; Li, J.; Chen, K.; Wang, W.; Li, Y.; et al. Nongrowing Season CO<sub>2</sub> Emissions Determine the Distinct Carbon Budgets of Two Alpine Wetlands on the Northeastern Qinghai—Tibet Plateau. *Atmosphere* **2021**, *12*, 1695. <https://doi.org/10.3390/atmos12121695>

Academic Editors: Baojie He, Ayyoob Sharifi, Chi Feng and Jun Yang

Received: 24 November 2021  
 Accepted: 15 December 2021  
 Published: 17 December 2021

**Publisher's Note:** MDPI stays neutral with regard to jurisdictional claims in published maps and institutional affiliations.



**Copyright:** © 2021 by the authors. Licensee MDPI, Basel, Switzerland. This article is an open access article distributed under the terms and conditions of the Creative Commons Attribution (CC BY) license (<https://creativecommons.org/licenses/by/4.0/>).

**Abstract:** Alpine wetlands sequester large amounts of soil carbon, so it is vital to gain a full understanding of their land-atmospheric CO<sub>2</sub> exchanges and how they contribute to regional carbon neutrality; such an understanding is currently lacking for the Qinghai—Tibet Plateau (QTP), which is undergoing unprecedented climate warming. We analyzed two-year (2018–2019) continuous CO<sub>2</sub> flux data, measured by eddy covariance techniques, to quantify the carbon budgets of two alpine wetlands (Luanhaizi peatland (LHZ) and Xiaobohu swamp (XBH)) on the northeastern QTP. At an 8-day scale, boosted regression tree model-based analysis showed that variations in growing season CO<sub>2</sub> fluxes were predominantly determined by atmospheric water vapor, having a relative contribution of more than 65%. Variations in nongrowing season CO<sub>2</sub> fluxes were mainly controlled by site (categorical variable) and topsoil temperature ( $T_s$ ), with cumulative relative contributions of 81.8%. At a monthly scale, structural equation models revealed that net ecosystem CO<sub>2</sub> exchange (NEE) at both sites was regulated more by gross primary productivity (GPP), than by ecosystem respiration (RES), which were both in turn directly controlled by atmospheric water vapor. The general linear model showed that variations in nongrowing season CO<sub>2</sub> fluxes were significantly ( $p < 0.001$ ) driven by the main effect of site and  $T_s$ . Annually, LHZ acted as a net carbon source, and NEE, GPP, and RES were  $41.5 \pm 17.8$ ,  $631.5 \pm 19.4$ , and  $673.0 \pm 37.2$  g C/(m<sup>2</sup> year), respectively. XBH behaved as a net carbon sink, and NEE, GPP, and RES were  $-40.9 \pm 7.5$ ,  $595.1 \pm 15.4$ , and  $554.2 \pm 7.9$  g C/(m<sup>2</sup> year), respectively. These distinctly different carbon budgets were primarily caused by the nongrowing season RES being approximately twice as large at LHZ ( $p < 0.001$ ), rather than by other equivalent growing season CO<sub>2</sub> fluxes ( $p > 0.10$ ). Overall, variations in growing season CO<sub>2</sub> fluxes were mainly controlled by atmospheric water vapor, while those of the nongrowing season were jointly determined by site attributes and soil temperatures. Our results highlight the different carbon functions of alpine peatland and alpine swampland, and show that nongrowing season CO<sub>2</sub> emissions should be taken into full consideration when upscaling regional carbon budgets. Current and predicted marked winter warming will directly stimulate increased CO<sub>2</sub> emissions from alpine wetlands, which will positively feedback to climate change.

**Keywords:** CO<sub>2</sub> fluxes; boosted regression trees; structural equation models; alpine wetlands; Qinghai—Tibet Plateau

## 1. Introduction

Due to their water-logged and relatively low-temperature conditions, wetlands comprise a large component of global terrestrial carbon reserves; they store ~30% of the global soil carbon pool, despite only constituting ~5% of the land surface [1–3]. Although pristine alpine wetlands could be potential future carbon sources because of the projected warming and drying climate [1,4,5], carbon accumulation in mid- and high-latitude wetlands has increased slightly over recent decades [2,6]. Thus, increased knowledge of carbon dynamics and their responses to environmental controls in alpine wetlands is essential to address this discrepancy and to quantify the contributions of wetlands in mitigating atmospheric greenhouse gas concentrations [4,7,8].

Alpine wetlands can be either carbon sources or carbon sinks depending on local hydrothermal conditions, consequent vegetation types, soil physical and chemical properties, and microorganism compositions [9–12]. Gross primary productivity (GPP) and ecosystem respiration (RES) are two contrasting processes that determine carbon budgets, and those are closely related to ecohydrological factors, usually with nonlinear relationships [13–15]. Water availability has been shown to be an important control of the seasonal variability in CO<sub>2</sub> fluxes of alpine wetlands, through its simultaneous effects on vegetation growth and organic matter decomposition [4,9,16]. Vascular plant coverage has an asymptotic relationship with GPP, and an incremental relationship with RES, but their sensitivity varies by leaf area index and vegetation type [17,18]. Under the context of climate warming scenarios, recent studies have shown that plant productivity outweighs ecosystem respiration, and alpine peatlands have become more efficient carbon sinks because of a higher sensitivity of GPP compared to RES, longer growing season, and more plant carbon input [19–21]. Contrarily, other studies have suggested that decreased moisture availability caused by warming could stimulate more soil respiration and potentially reverse the carbon sink function [6,22,23]. Quantifying the relative contributions of biotic and abiotic controls on carbon budgets has the potential to understand this debate but has been poorly addressed because of their intertwined relationships [22]. Moreover, nongrowing season CO<sub>2</sub> emissions are believed to play a considerable role in carbon budgets, but there is still much uncertainty due to limited long-term field observations [4,18]. More detailed knowledge is greatly needed to quantify and predict the fate of the carbon function of alpine wetlands under remarkable winter warming and increasing precipitation [9,13]. Year-round continuous measurements, rather than merely from the growing season, are required in alpine wetlands to address this issue [23,24].

Carbon budgets of alpine wetlands on the Qinghai—Tibet Plateau (QTP) have drawn increased attention recently [11,13,25,26]; the QTP wetlands house relatively large soil carbon reservoirs because of lower decomposition rates and higher vegetation photosynthetic production compared with other surrounding wetland ecosystems [4,17]. Moreover, wetlands on the QTP have been expanding due to the warming climate and decreased human activity [27]. However, the carbon sink/source functions in alpine wetlands are highly variable. For instance, the wetlands of Zoige, Qinghai Lake (Xiaobohu: XBH), and Hehei have recently behaved as carbon sinks, with annual carbon accumulations of approximately 170, 250, and 510 g C/m<sup>2</sup>, respectively [12,13,28]. In contrast, Luanhaizi (LHZ) wetland has been a carbon source and released approximately 100 g C/(m<sup>2</sup> year) to the atmosphere from 2005 to 2014 [14,17,25]. Therefore, quantifying the carbon dynamics of contrasting alpine wetlands will be helpful in understanding the confounding mechanisms in their carbon budgets. In this study, we obtained CO<sub>2</sub> fluxes and auxiliary environmental variables, measured by eddy covariance systems, over a two-year period from 2018 to 2019, from both LHZ and XBH on the northeastern QTP (Figure S1). This enables us to quantify

inter-seasonal and inter-annual CO<sub>2</sub> budgets of the two contrasting alpine wetlands and to explore the relative contributions of each of the main environmental controls and their underlying ecological processes. We hypothesize that RES will contribute more than GPP to the distinct carbon functions of the two wetlands, because prior studies have reported that annual GPP was nearly equivalent in these two wetlands (630 g C/m<sup>2</sup> in LHZ [17] and 640 g C/m<sup>2</sup> in XHB [29]).

## 2. Materials and Methods

### 2.1. Site Descriptions

The two alpine wetlands, namely Luanhaizi (LHZ, 37°35' N, 101°20' E, 3250 m altitude) and Xiaobohu (XBH, 36°42' N, 100°47' E, 3210 m altitude), are both located on the northeastern Qinghai—Tibet Plateau (Figure S1); these can be classified as peatland and swampland, respectively, according to the differences in vegetation community, hydrological processes, and soil history [27]. The climate is cold and humid, belonging to the plateau monsoon climate of the alpine, frigid temperate zone.

LHZ lies adjacent to the Haibei National Field Research Station for Alpine Grasslands, which is a long-standing member of the Chinese Flux Observation and Research Network (ChinaFLUX). XBH lies on the eastern Qinghai Lake and belongs to the Qinghai Normal University. The mean annual air temperature and precipitation were −1.1 °C and 490.0 mm in LHZ [17], respectively, and 1.2 °C and 357.0 mm in XBH [29]. The 0–20 cm soil organic carbon content averaged 15.7% at LHZ and 6.2% at XBH. In LHZ, the dominant plant species were *Kobresia tibetica*, *Carex pamirensis*, *C. alofusca*, *Blysmus sinocompressus*, *Hippuris vulgaris*, and *Triglochin palustre* [14]. The relative vegetation coverage, aboveground biomass, and belowground biomass during the flourishing growth stage (July–August) were approximately 95%, 340 g/m<sup>2</sup>, and 4200 g/m<sup>2</sup>, respectively [25]. LHZ was constantly submerged during the growing season, and the water depth was about 20 cm, with remarkable spatial and temporal variations [9]. In XBH, the dominant plant species were *C. limosa*, *B. sinocompressum*, *K. tibetica*, *Schoenoplectus tabernaemontani*, and *Phragmites australis*. The relative vegetation coverage, aboveground biomass, and belowground biomass from July to August averaged 85%, 225 g/m<sup>2</sup>, and 3200 g/m<sup>2</sup>, respectively. The maximum volumetric topsoil water content was about 60% [29].

### 2.2. Measurements

CO<sub>2</sub> fluxes were measured by eddy covariance techniques at both sites. An eddy flux tower, including a three-dimensional ultrasound anemometer (CSAT3, the offset error < ± 8.0 cm/s, Campbell Scientific, Logan, UT, USA) and an open-path infrared CO<sub>2</sub>/H<sub>2</sub>O analyzer (Li-7500 for LHZ and Li-7500A for XBH, the typical zero drift was ± 0.1 ppm in CO<sub>2</sub> and ± 0.03 mmol/mol in H<sub>2</sub>O, Li-Cor, Lincoln, NE, USA), was installed at a height of approximately 2.0 m above the surface; these have been in place since 2003 in LHZ and since 2010 in XBH. The raw data frequency was 10 Hz. A micro-meteorology station was also constructed adjacent to the flux tower, to monitor air temperature, atmospheric water vapor, wind speed and direction, four-component radiation, precipitation, and topsoil temperature. More detailed measurement information can be found in prior papers [17,29]. The growing season was simply defined as May–October for both sites and was robust because the enhanced vegetation index was above 0.2 during these periods (Figure 1f).

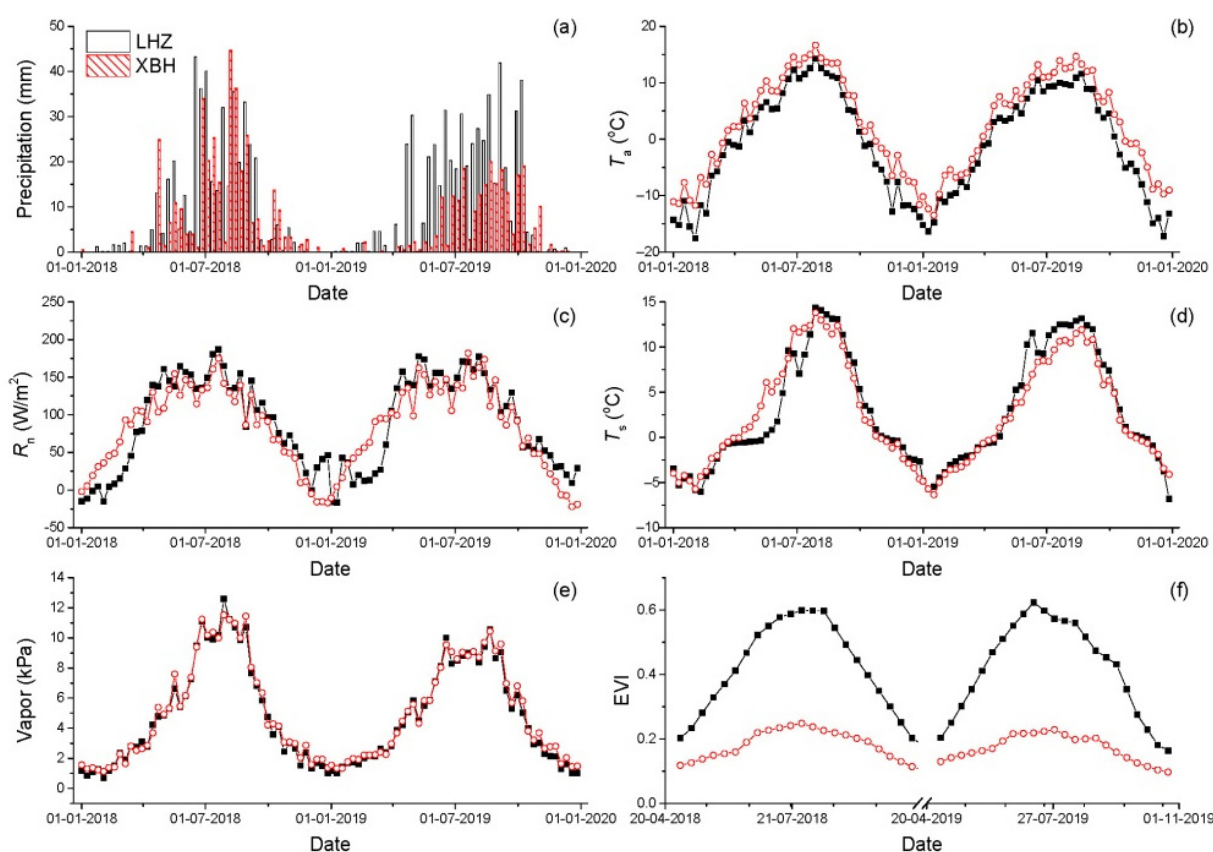


**Figure 1.** The seasonal variations in precipitation (a), air temperature ( $T_a$ ), (b), net radiation ( $R_n$ ), (c), topsoil temperature ( $T_s$ ), (d), atmospheric water vapor (Vapor), (e) and enhanced vegetation index (EVI), (f) from 2018 to 2019 at the two alpine wetlands.

### 2.3. Data Collection and Processing

Subsequent to raw high-frequency data collection, half-hour  $\text{CO}_2$  fluxes were computed from spike removal, two-dimensional coordinate rotation, time-lag compensation, and the Webb-Pearman-Leuning (WPL) ‘Burba correction’ for density fluctuations because of the self-heating effect [30] using Eddypro 7.0.6 (Li-Cor, Lincoln, NE, USA). The calculated  $\text{CO}_2$  fluxes were screened to improve data quality by removal of a quality flag with “2” [31] and outliers (beyond 4.5 standard deviations) in a 10-day window, and by filtering against lower turbulence (threshold nighttime friction velocity was  $0.15 \text{ m s}^{-1}$ ). The annual valid data coverage was  $\sim 40\%$ , with  $\sim 70\%$  and  $\sim 20\%$  in the daytime and nighttime, respectively, comparable to data reported for ChinaFLUX [32] and other alpine sites [22]. The  $\text{CO}_2$  flux data were gap-filled by a machine learning algorithm of boosted regression trees (BRT) [33], which was conducted using a dataset with a valid flux subset and corresponding routine meteorological subset, including air temperature, atmospheric water vapor, net radiation, wind velocity, and topsoil temperature. Machine learning algorithms were found to outperform other conventional gap-filling techniques by incorporating all of the main environmental controls simultaneously [34,35]. Because of the distinctly different processes governing  $\text{CO}_2$  exchanges between growing season daytime (Growing: the simultaneous occurrence of plant photosynthesis and ecosystem respiration) and nongrowing season all-time and growing season nighttime (Nongrowing: only ecosystem respiration occurred), we filled data gaps separately. Firstly, boosted regression trees were fitted using the Growing valid dataset (BRT-growing) and the Nongrowing valid dataset (BRT-nongrowing), respectively. Secondly, the fitted BRT-growing and BRT-nongrowing, respectively, were used to fill data gaps with corresponding meteorological variables. After several comparisons, tree complexity, learning rate, and number of trees in BRT were fixed at 5, 0.005, and 5000, respectively.

The growing season daytime ecosystem respiration was estimated from the nongrowing-BRT and extrapolated based on the daytime meteorological variables. Therefore, daily ecosystem respiration (RES) is the sum of daytime respiration and nocturnal respiration. Daily GPP equals the values that daily RES minus daily NEE.

The enhanced vegetation index (EVI, MYD13Q1) was adopted as a metric for capturing the relationship between CO<sub>2</sub> fluxes and biotic variables in alpine grasslands [35–37]. The 8-day EVI was flux tower-centric at 500 × 500 m spatial resolution and was obtained from the Oak Ridge National Laboratory Distributed Active Archive Center (ORNL DAAC, <https://modis.ornl.gov/globalsubset/>). Half-hour values of CO<sub>2</sub> fluxes and meteorological variables were aggregated into an 8-day scale to match the temporal resolution of the EVI.

#### 2.4. Statistical Analysis

BRT is well documented for ecological studies [33–35] and was here adopted to explore the relative contributions to 8-day CO<sub>2</sub> fluxes of the main environmental controls, which included continuous variables (air temperature, atmospheric water vapor, wind speed, net radiation, topsoil temperature, and enhanced area index) and categorical variables (site name, indicative site attributes). Vapor pressure deficit (VPD) can also represent atmospheric moisture status but was excluded from the key environmental controls because of its limited contribution to variations in CO<sub>2</sub> fluxes (Figure S2) in alpine grasslands [35]. More importantly, this algorithm can tolerate collinearity and nonnormality among environmental controls, which are rather common in environmental studies. Piecewise structural equation models (SEM) were used to identify the total effects and pathways of environmental controls on monthly CO<sub>2</sub> fluxes. BRT and SEM were performed by the package of “Dismo” [33] and “piecewiseSEM” [38] in R 4.0.3 [39]. Other conventional statistical analysis, such as linear regression, correlative analysis, and general linear models were also conducted in R.

### 3. Results

#### 3.1. Information Regarding Abiotic and Biotic Controls

The two wetlands experienced small differences in climate during the two study years, with LHZ being relatively wetter and colder (Figure 1). Annual precipitation averaged 487.8 mm at LHZ and 291.8 mm at XBH. Annual mean air temperature ( $T_a$ ) was  $-0.9$  °C at LHZ, which was lower than that of XBH by 3.3 °C. Mean daily net radiation ( $R_n$ ) was almost equivalent, being approximately 85.0 W/m<sup>2</sup> at both locations. Annual mean topsoil temperature ( $T_s$ ) and atmospheric water vapor were also similar at the two wetlands, and averaged 2.7 °C and 4.9 kPa, respectively. Vapor pressure deficit (VPD) was 0.26 kPa in LHZ and 0.39 kPa in XBH. However, there was a distinct difference in EVI, with an annual value of 0.40 at LHZ and 0.17 at XBH. The maximum 8-day EVI was approximately 0.62 at the end of July in LHZ, which was over twice more than that of XBH (0.25; Figure 1).

#### 3.2. Eight-Day Variations in CO<sub>2</sub> Fluxes

The trends of seasonal CO<sub>2</sub> fluxes were similar at the two sites, although the magnitudes were to some extent different (Figure 2). Daily GPP averaged  $3.23 \pm 1.88$  g C/(m<sup>2</sup> d) (Mean ± S.D., the same below) at LHZ and  $3.43 \pm 2.25$  g C/(m<sup>2</sup> d) at XBH. The paired-sample t-test showed that the difference was marginally significant ( $p = 0.07$ ). Daily RES was  $1.83 \pm 0.90$  g C/(m<sup>2</sup> d) at LHZ, which was significantly ( $p < 0.001$ ) more (by 17.6%) than that of XBH. Therefore, daily NEE was  $0.11 \pm 1.57$  g C/(m<sup>2</sup> d) at LHZ, and this was much higher than that of XBH ( $-0.11 \pm 0.96$  g C/(m<sup>2</sup> d)).

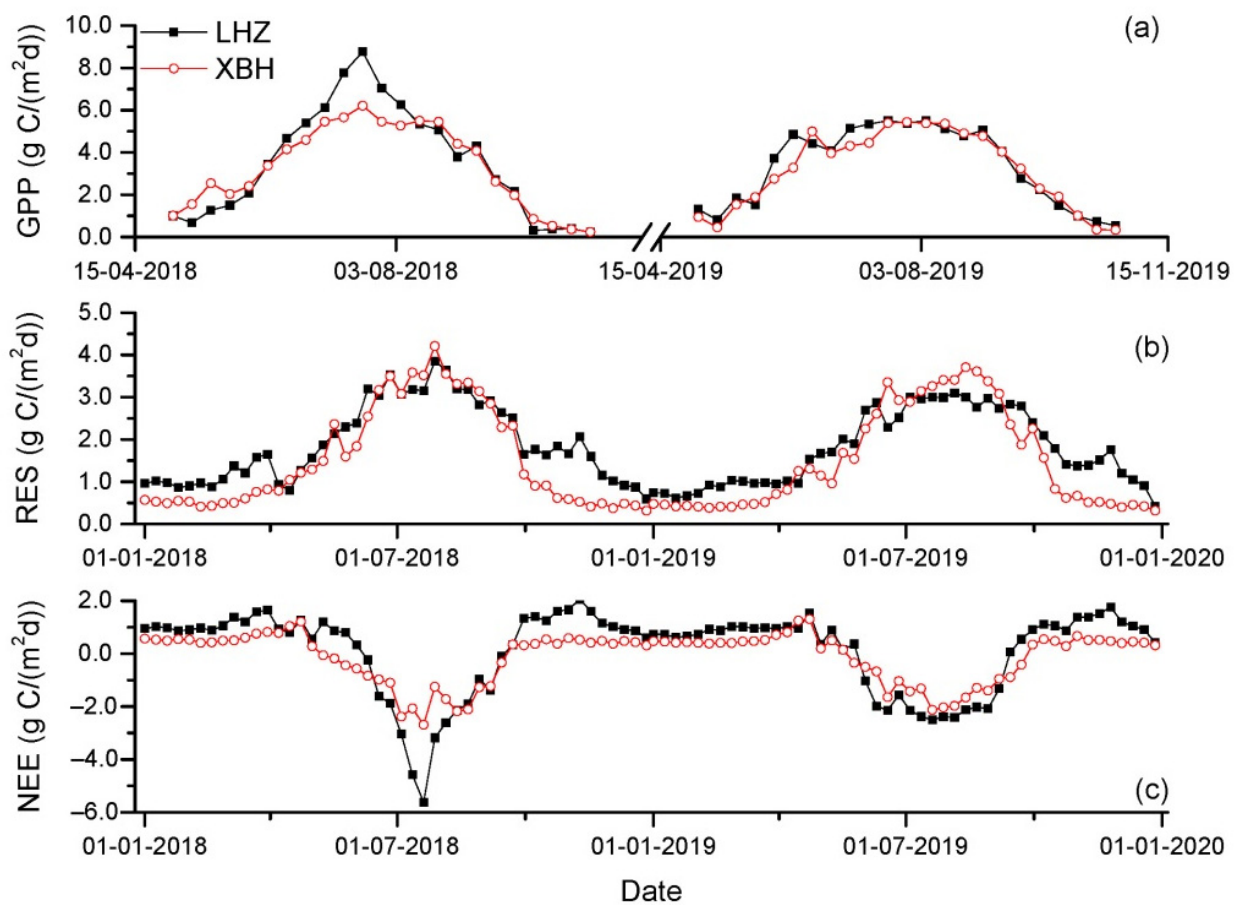


**Figure 2.** The 8-day variations in CO<sub>2</sub> fluxes of the two alpine wetlands (gross primary productivity GPP, (a); ecosystem respiration RES, (b); net ecosystem CO<sub>2</sub> exchange NEE, (c)).

During the growing season, the mean total deviance and 10-fold cross-validation deviance for 8-day GPP, RES, and NEE were 108.57 and 9.67, 72.14 and 3.47, and 269.57 and 17.64, respectively, which suggested the good performance of the BRT models ( $R^2 > 0.90$ , Figure S3). The results showed that the variations of 8-day GPP and 8-day NEE were mostly determined by atmospheric water vapor, with relative contributions of more than 65% (Figure 3a). GPP showed a positive correlation with atmospheric water vapor, while NEE showed a negative correlation with atmospheric water vapor (Figure 4a,d). Variations in 8-day RES were jointly controlled by atmospheric water vapor and  $T_s$ , which explained 76.5% of the total variations. RES showed a positive correlation with both atmospheric water vapor and  $T_s$  (Figure 4b,c). It should be noted that the relative contribution of site (categorical variables) was less than 2%, which indicated that the growing season patterns of 8-day CO<sub>2</sub> fluxes at the two sites should be attributed to variations in environmental controls rather than site attributes. Furthermore, the contribution of EVI to NEE was more than 10%, although it was only 5.0% for GPP and 9.8% for RES (Figure 3a).

During the nongrowing season, the mean total deviance and 10-fold cross-validation deviance for 8-day NEE were 9.57 and 2.59 ( $R^2 = 0.73$ ; Figure S3), respectively. The variability in NEE was jointly determined by site attributes and  $T_s$ , with cumulative relative contributions of 81.8% (Figure 3b). Mean daily NEE was approximately  $1.07 \pm 1.57$  g C/(m<sup>2</sup> d) at LHZ, which was about twice that of XBH ( $0.56 \pm 0.96$  g C/(m<sup>2</sup> d), Figure 4e). NEE exponentially increased with  $T_s$  at both sites (Figure 4f).

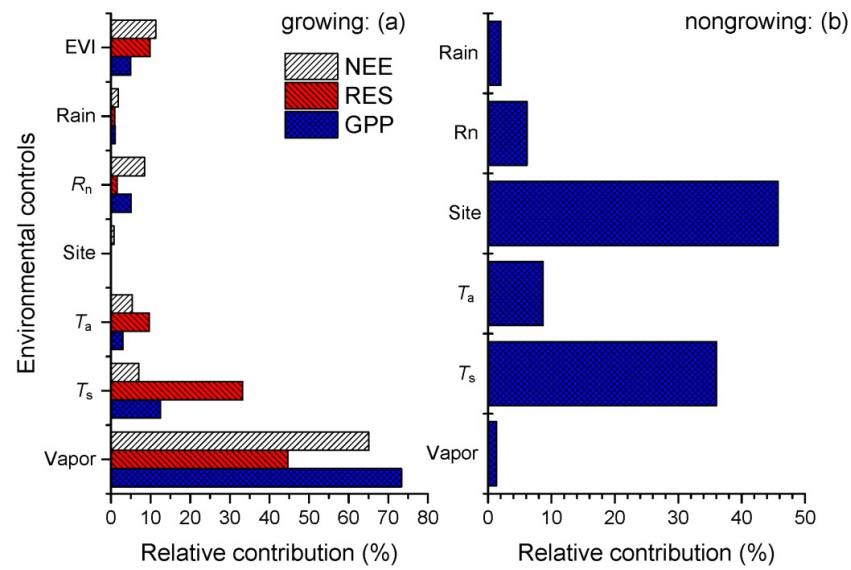


**Figure 3.** The relative contributions of environmental controls on variations in the growing season (a) and the nongrowing season (b) 8-day CO<sub>2</sub> fluxes of the two alpine wetlands.

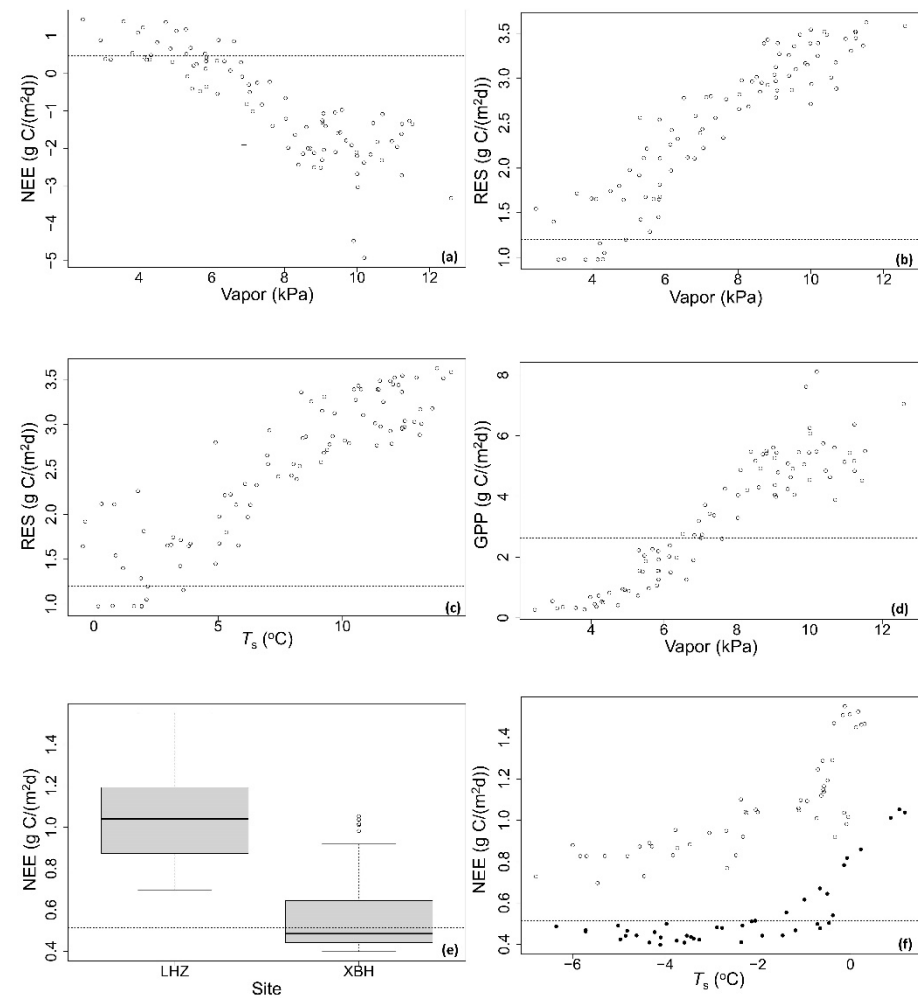


**Figure 4.** The fitted 8-day CO<sub>2</sub> fluxes (net ecosystem exchange NEE, (a,e,f) ecosystem respiration RES, (b,c) gross primary productivity GPP, (d) in relation to each of the important predictors (Vapor: atmospheric water vapor; T<sub>s</sub>: topsoil temperature) used in the model during the growing season (a,d) and nongrowing season (e,f).

### 3.3. Monthly Variations in CO<sub>2</sub> Fluxes

Maximum monthly GPP occurred in July and August at both sites (Figure 5), and averaged  $179.6 \pm 28.0$  g C/(m<sup>2</sup> month) at LHZ and  $161.6 \pm 11.0$  g C/(m<sup>2</sup> month) at XBH. Similarly, maximum monthly RES averaged  $97.2 \pm 6.0$  g C/(m<sup>2</sup> month) at LHZ and  $105.2 \pm 5.8$  g C/(m<sup>2</sup> month) at XBH during July and August. The minimum monthly NEE averaged  $-82.4 \pm 24.3$  g C/(m<sup>2</sup> month) at LHZ and  $-56.4 \pm 7.3$  g C/(m<sup>2</sup> month) at XBH during these two months. Interestingly, the maximum monthly NEE occurred in November ( $47.5 \pm 3.2$  g C/(m<sup>2</sup> month)) at LHZ, while it occurred in April ( $30.3 \pm 1.4$  g C/(m<sup>2</sup> month)) at XBH, reflecting different hydrothermal conditions. The monthly RES at LHZ ( $56.1 \pm 27.2$  g C/(m<sup>2</sup> month)) was significantly ( $p < 0.001$ ) more than that at XBH ( $46.2 \pm 35.7$  g C/(m<sup>2</sup> month)), in contrast to the undetectable difference in monthly GPP ( $p = 0.23$ ) and monthly NEE ( $p = 0.10$ ) at the two sites (Figure 6). Further analysis showed that the difference of RES mainly stemmed from an approximately two-fold larger non-growing season RES at LHZ (Figure 6b). Moreover, the nongrowing season RES comprised as much as 29.5% of the annual RES in LHZ, but only comprised 18.5% in XBH.

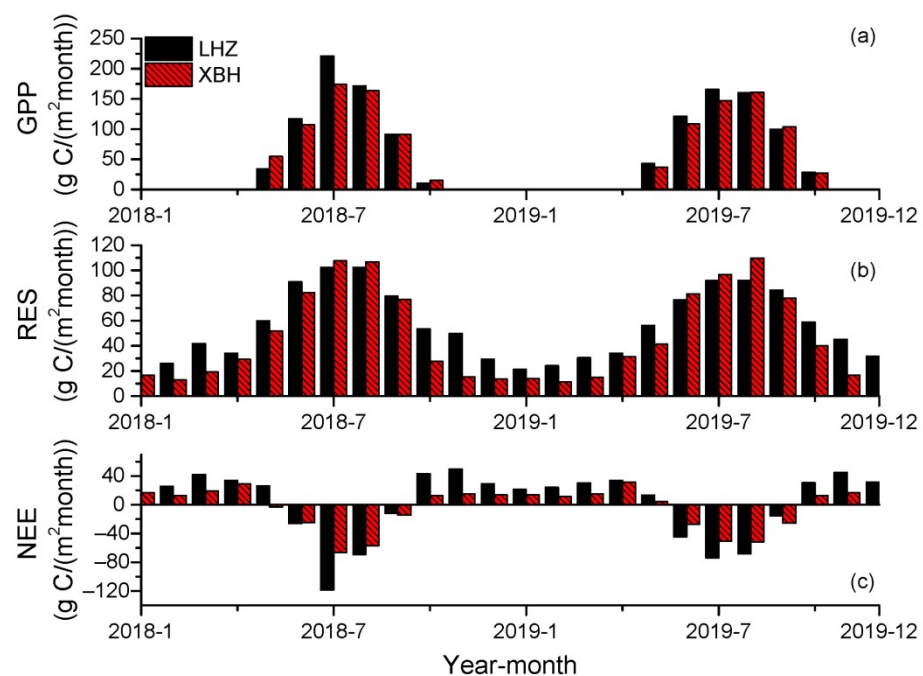


**Figure 5.** The monthly variations in CO<sub>2</sub> fluxes of the two alpine wetlands (gross primary productivity GPP, (a); ecosystem respiration RES, (b); net ecosystem CO<sub>2</sub> exchange NEE, (c)).

During the growing season, both NEE and RES were significantly correlated with GPP, with 69.0% of the per-unit GPP contributed to RES and 31.0% to NEE. Monthly NEE at both sites was controlled much more by monthly GPP than by monthly RES, indicated by stronger standardized coefficients for the former (Figure 7). GPP and RES were both controlled by atmospheric water vapor and the direct effect was similar for both LHZ and XBH (0.78 versus 0.79 for GPP, and 1.01 versus 0.96 for RES) for the two wetlands. It should be noted that the indirect effect of atmospheric water vapor through EVI on CO<sub>2</sub> fluxes was significant ( $p < 0.05$ ) at XBH alone, and the total effects of atmospheric water vapor on GPP and RES were 1.19 ( $0.79 + 1.09 \times 0.37$ ) and 1.07 ( $0.79 + 1.09 \times 0.26$ ), respectively (Figure 7b). This might be caused by XBH being a much lower EVI (Figure 1f). Therefore, the variations in monthly CO<sub>2</sub> fluxes were predominantly determined by monthly atmospheric water vapor during the growing season, and the effect of vegetation growth was important at XBH with lower plant coverage. GPP/RES, which evaluates the relative contribution of CO<sub>2</sub> exchange processes to the total CO<sub>2</sub> exchange, averaged  $1.21 \pm 0.61$  at LHZ and

$1.20 \pm 0.35$  at XBH, respectively. The paired-sample t-test showed that the difference in GPP/RES between the two sites was non-significant ( $p = 0.91$ ,  $N = 12$ ).

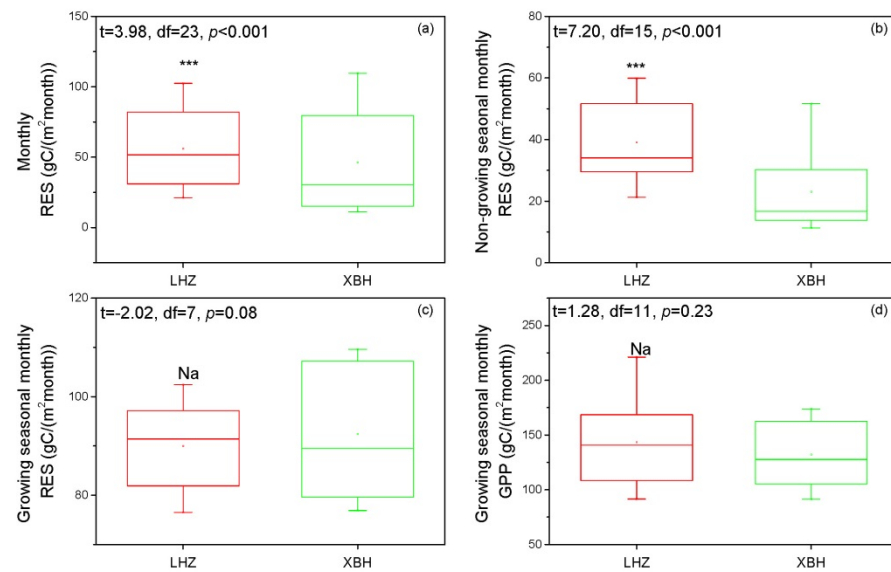


**Figure 6.** The paired-sample t-test on the monthly ecosystem respiration (RES) at the whole year (a), non-growing season (b), growing season (c) and the growing season monthly gross primary productivity (GPP), (d) of the two alpine wetlands (Na: non-significant; \*\*\*:  $p < 0.001$ ).

During the nongrowing season, monthly NEE was controlled by monthly  $T_s$ , and the relationship could be depicted by a  $Q_{10}$ -based model ( $NEE = a \times e^{\ln(Q_{10})(T_s-10)/10}$ ,  $Q_{10}$  describes the proportional increase in the rate of respiration per  $10^\circ\text{C}$  rise in temperature [5]; Figure 8). The reference respiration in LHZ was 29.8% more than that of XBH, while  $Q_{10}$  was 27.3% lower at the former site. Furthermore, the general linear model of monthly  $\ln(NEE)$  with  $T_s$  and site (categorical variable) revealed that the main effects of  $T_s$  and site attributes were both significant ( $p < 0.001$ ), but the interaction was insignificant ( $p = 0.91$ ; Table S1). Thus, the nongrowing season monthly NEE should be jointly determined by  $T_s$  and site attributes.

Fisher's C = 4.97, AIC=40.97, P= 0.55, df = 6

LHZ: (a)

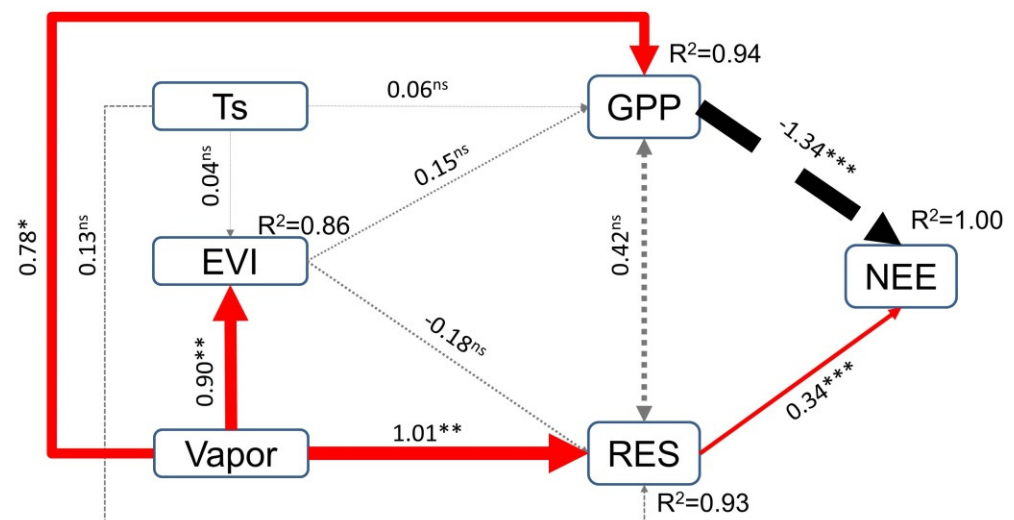


**Figure 7.** Cont.



related to annual accumulative EVI ( $p < 0.03$ ,  $N = 4$ ,  $R^2 > 0.94$ ; Table S2). Annually, the carbon use efficiency ( $-NEE/GPP$ ) averaged  $-0.065 \pm 0.026$  at LHZ and  $0.068 \pm 0.011$  at XBH, respectively.

## 4. Discussion

### 4.1. Environmental Controls on CO<sub>2</sub> Fluxes

The variations in growing season CO<sub>2</sub> fluxes were mainly determined by atmospheric water vapor in the two alpine wetlands (Figures 3 and 7), which is inconsistent with the long-standing view that thermal conditions predominantly control CO<sub>2</sub> fluxes in these temperature-limited wetlands [14,15,40]. There are two potential explanations for this finding from the perspectives of the atmospheric water vapor itself and plant physiology. First, atmospheric water vapor is an integral indicator of hydrothermal status and can exert a substantial influence on land carbon uptake variability through its indirect effects from soil moisture-atmosphere feedbacks [41,42]; this is indeed exponentially related to  $T_a$  (atmospheric water vapor =  $3.9e^{0.08T_a}$ ,  $R^2 = 0.97$ ,  $p < 0.001$ ) and  $T_s$  (atmospheric water vapor =  $2.6e^{0.11T_s}$ ,  $R^2 = 0.83$ ,  $p < 0.001$ ) and would, thus, be a reasonable proxy of thermal conditions. Second, the optimum temperature of plant physiological activity is closely related to the growing season air temperature due to long-term plant evolutionary adaptation [43]. In other words, current thermal conditions should be comparable for analogous plant photosynthesis and growth within a certain cold site [44,45]. Additionally, the effects of thermal conditions on CO<sub>2</sub> fluxes are markedly moisture-dependent, based on reports from warming experiments in alpine regions [45,46]. Thus, atmospheric water vapor should be a reliable metric of hydrothermal conditions controlling growing season CO<sub>2</sub> fluxes in alpine wetlands [12,35]. The nongrowing season CO<sub>2</sub> fluxes were jointly controlled by site attributes and  $T_s$  (Figures 3 and 8). This stems from the fact that ecosystem respiration consists of root autotrophic respiration and microbial heterotrophic respiration, which are closely related to substrate availability and soil temperatures in alpine regions [9,44]. Therefore, atmospheric water vapor, more than air/soil temperatures, regulated the variability in growing season CO<sub>2</sub> fluxes, while site attributes and soil temperatures jointly controlled nongrowing season CO<sub>2</sub> emissions in our wetlands. These findings are consistent with previous studies [4,12,18]. Given that the nongrowing season temperature is projected to further increase across the QTP [47], these alpine wetlands will likely release more carbon and positively feedback to climate change [5]; this prediction is different from the model simulations of a single site where little attention was paid to nongrowing season CO<sub>2</sub> dynamics [13,26].

### 4.2. Carbon Budgets of the Two Wetlands

The distinct carbon function of the two wetlands is explained more by RES, than by GPP, specifically by nongrowing RES (Figures 4 and 6). The smaller annual carbon use efficiency (about 6%) and little difference in growing GPP/RES (1.20) also confirmed the important role of nongrowing RES in carbon budgets. The nongrowing season daily CO<sub>2</sub> effluxes were  $1.07 \text{ g C}/(\text{m}^2 \text{ d})$  in LHZ and  $0.56 \text{ g C}/(\text{m}^2 \text{ d})$  in XBH, which lie within the reported values of other alpine wetlands [4,40]. The higher nongrowing season RES at LHZ compared to XBH thus contributed to a net carbon source at LHZ. Soil temperature was similar at both sites (Figure 1) and was still high enough to support organic matter decomposition and root respiration due to the snow insulation effect, despite the air temperature being below  $-10 \text{ }^\circ\text{C}$  [4,16]; hence, greater root biomass and more soil organic carbon at LHZ, rather than thermal conditions, probably led to more ecosystem respiration at LHZ compared to XBH during the nongrowing season [1,4]. Meanwhile, the easily degradable labile carbon from plant litter, induced by higher vegetation coverage (e.g., two-fold higher EVI at LHZ), will stimulate enhanced microbial growth, carbon mineralization, and soil respiration at LHZ [11]. However, the temperature sensitivity of RES was much higher at XBH (Figure 8), which also indicated lower stability of soil organic matter at this site [21].

The nonsignificant difference in GPP possibly stems from the higher productivity of swampland plants compared to peatland plants [9]. This appears to be confirmed by a three-fold higher sensitivity of GPP to EVI (slope = 40.5 g C/(m<sup>2</sup> d)) at XBH compared to that at LHZ (slope = 14.5 g C/(m<sup>2</sup> d)). The growing season RES was closely correlated with GPP ( $R^2 > 0.90$ ,  $p < 0.001$ ; Figure S4) at both sites, through substrate supply [13]. Therefore, nonsignificant GPP results in little difference in growing season plant autotrophic respiration and the consequent RES, specifically, nongrowing season RES contributes to the distinct carbon functions in the two alpine wetlands.

Higher carbon sink capacity appears to coincide with higher precipitation, which is in agreement with previous reports from alpine wetlands [14,19,40]. However, the underlying responses of the two sites are clearly different. Greater precipitation inhibited carbon dynamics at LHZ while stimulated carbon exchanges at XBH (Figure S5). Specifically, at LHZ, the higher precipitation (536.1 mm versus 439.6 mm) decreased annual GPP less by 27.5 g C/m<sup>2</sup> (645.2 g C/(m<sup>2</sup> year) versus 617.7 g C/(m<sup>2</sup> year)), compared to a decrease in RES of 52.6 g C/m<sup>2</sup> (699.3 g C/(m<sup>2</sup> year) versus 646.7 g C/(m<sup>2</sup> year)). Decreased carbon fluxes might be caused by more waterlogged patches and lower oxygen availability for soil respiration under higher precipitation [14,17,23]. At XBH, the greater precipitation (238.8 mm versus 344.7 mm) stimulated increased GPP by 21.8 g C/m<sup>2</sup> (584.2 g C/(m<sup>2</sup> year) versus 606.0 g C/(m<sup>2</sup> year)), compared to an increase in RES of 11.1 g C/m<sup>2</sup> (548.7 g C/(m<sup>2</sup> year) versus 559.8 g C/(m<sup>2</sup> year)). Such a phenomenon indicates that GPP and RES at XBH should be to some extent water-stressed, which agrees well with previously reported positive relationships between CO<sub>2</sub> fluxes and water availability at the same site from 2012 to 2013 [29]. Indeed, recent studies have suggested that the response of soil carbon decomposition to water-table manipulation in LHZ is controlled by ferrous iron, in contrast to the classic “enzyme latch” theory seen in other wetlands [21,48]. Therefore, the different responses of CO<sub>2</sub> fluxes to promoted precipitation between peatlands and swamplands should be taken into full consideration in predicting the feedback of alpine wetlands to climate change on the QTP. Further, more extensive and long-term studies, including those on another potent greenhouse gas, CH<sub>4</sub>, are required to quantify the contribution of alpine wetlands to the regional carbon neutrality of alpine wetlands [8].

## 5. Conclusions

Using two-year continuous measurements from the northeastern Qinghai—Tibet Plateau, this study revealed that an alpine peatland site acted as a net carbon source, while an alpine swampland site acted as a net carbon sink. Growing season CO<sub>2</sub> fluxes were predominantly controlled by atmospheric water vapor, while nongrowing season ecosystem respiration was regulated by site attributes and topsoil temperatures. Ecosystem respiration, specifically nongrowing season CO<sub>2</sub> emissions, potentially accounted for the distinctly different carbon budgets of the two alpine wetlands. These findings highlight the crucial role of nongrowing season CO<sub>2</sub> dynamics in alpine wetlands, which will positively feedback to climate change under the context of marked winter warming.

**Supplementary Materials:** The following are available online at <https://www.mdpi.com/article/10.3390/atmos12121695/s1>, Table S1: The analysis of variance from the general linear model of monthly net ecosystem exchange ( $\ln(NEE)$ ) with soil temperature ( $T_s$ , continuous variable) and site attributes (Site, categorical variable) during the nongrowing season, Table S2: The Pearson correlation analysis between annual CO<sub>2</sub> fluxes (NEE, RES, GPP) with environmental controls ( $T_a$ : air temperature; Vapor: atmospheric water vapor; Rain: precipitation;  $R_n$ : net radiation;  $T_s$ : topsoil temperature;  $EVI_{sum}$ : accumulative enhanced vegetation index). Figure S1: The geographic location of the two alpine wetlands, Figure S2: The relative contributions of environmental controls to variations in the growing season (a) and the nongrowing season (b) 8-day CO<sub>2</sub> fluxes of the two alpine wetlands, Figure S3: The fitted 8-day CO<sub>2</sub> fluxes (NEE: (a, d); RES (b); GPP (c)) in relation to each of the predictors (Rain: precipitation;  $T_a$ : air temperature;  $R_n$ : net radiation; Vapor: atmospheric water vapor;  $T_s$ : topsoil temperature; EVI: enhanced vegetation index; Site: categorical variable, LHZ and XBH) used in the model during the growing season (a, b, c) and nongrowing season (d), Figure S4: The relationship

between monthly ecosystem respiration (RES) and monthly gross primary productivity (GPP) during the growing season of the two alpine wetlands (LHZ: Luanhaizi and XBH: Xiaobohu). The shading areas are 95% confidence intervals, Figure S5: The relationships of annual carbon fluxes and annual precipitation of the two alpine wetland sites (Xiaobohu: XBH and Luanhaizi: LHZ).

**Author Contributions:** Conceptualization, F.Z. and W.W.; methodology, C.S., F.L., L.Z., C.W. and Y.L.; software, C.S. and F.Z.; validation, C.S., L.Y. and J.L.; investigation, C.S., F.L., Y.Y. and L.Z.; resources, K.C. and Y.L.; supervision, F.Z.; funding acquisition, F.Z., K.C., W.W. and Y.L. All authors have read and agreed to the published version of the manuscript.

**Funding:** This work is funded by the Chinese Academy of Sciences–People’s Government of Qinghai Province Joint Grant on Sanjiangyuan National Park Research (LHZX-2020-07, LHZX-2020-08), the project of Economic Development Research Center of National Forestry and Grassland Administration (JYFL-2021-20); the National Key R&D Program (2017YFA0604802), the National Natural Science Foundation of China (41877547), the 2021 first funds for central government to guide local science and technology development in Qinghai Province (2021ZY002), and the Second Tibetan Plateau Scientific Expedition and Research (STEP) Program (2019QZKK0302).

**Institutional Review Board Statement:** Not applicable.

**Informed Consent Statement:** Not applicable.

**Data Availability Statement:** The data are available on reasonable request to the corresponding author.

**Conflicts of Interest:** The authors declare no conflict of interest.

## Abbreviations

BRT: boosted regression trees; SEM: structural equation model; EVI: enhanced area index; Rain: precipitation;  $R_n$ : net radiation;  $T_a$ : air temperature;  $T_s$ : topsoil temperature; Vapor: atmospheric water vapor; VPD: vapor pressure deficit; NEE: net ecosystem CO<sub>2</sub> exchange; GPP: gross primary productivity; RES: ecosystem respiration; LHZ: Luanhaizi peatland; XBH Xiaobohu swampland; ChinaFLUX: Chinese Flux Observation and Research Network; QTP: Qinghai–Tibet Plateau.

## References

1. Limpens, J.; Berendse, F.; Blodau, C.; Canadell, J.G.; Freeman, C.; Holden, J.; Roulet, N.; Rydin, H.; Schaepman-Strub, G. Peatlands and the carbon cycle: From local processes to global implications—A synthesis. *Biogeosciences* **2008**, *5*, 1475–1491. [[CrossRef](#)]
2. Mitsch, W.J.; Bernal, B.; Nahlik, A.M.; Mander, Ü.; Zhang, L.; Anderson, C.J.; Jørgensen, S.E.; Brix, H. Wetlands, carbon, and climate change. *Landsc. Ecol.* **2013**, *28*, 583–597. [[CrossRef](#)]
3. Yu, Z.; Loisel, J.; Brosseau, D.P.; Beilman, D.W.; Hunt, S.J. Global peatland dynamics since the Last Glacial Maximum. *Geophys. Res. Lett.* **2010**, *37*, L13402. [[CrossRef](#)]
4. Pullens, J.W.M.; Sottocornola, M.; Kiely, G.; Toscano, P.; Gianelle, D. Carbon fluxes of an alpine peatland in Northern Italy. *Agric. For. Meteorol.* **2016**, *220*, 69–82. [[CrossRef](#)]
5. Dise, N.B. Peatland Response to Global Change. *Science* **2009**, *326*, 810. [[CrossRef](#)] [[PubMed](#)]
6. Gallego-Sala, A.V.; Charman, D.J.; Brewer, S.; Page, S.E.; Prentice, I.C.; Friedlingstein, P.; Moreton, S.; Amesbury, M.J.; Beilman, D.W.; Björck, S.; et al. Latitudinal limits to the predicted increase of the peatland carbon sink with warming. *Nat. Clim. Change* **2018**, *8*, 907–913. [[CrossRef](#)]
7. Lund, M.; Lafleur, P.M.; Roulet, N.T.; Lindroth, A.; Christensen, T.R.; Aurela, M.; Chojnicki, B.H.; Flanagan, L.B.; Humphreys, E.R.; Laurila, T.; et al. Variability in exchange of CO<sub>2</sub> across 12 northern peatland and tundra sites. *Glob. Chang. Biol.* **2010**, *16*, 2436–2448. [[CrossRef](#)]
8. Wei, D.; Zhao, H.; Huang, L.; Qi, Y.; Wang, X. Feedbacks of Alpine Wetlands on the Tibetan Plateau to the Atmosphere. *Wetlands* **2020**, *40*, 787–797. [[CrossRef](#)]
9. Hirota, M.; Tang, Y.; Hu, Q.; Hirata, S.; Kato, T.; Mo, W.; Cao, G.; Mariko, S. Carbon Dioxide Dynamics and Controls in a Deep-water Wetland on the Qinghai-Tibetan Plateau. *Ecosystems* **2006**, *9*, 673–688. [[CrossRef](#)]
10. Xiao, D.; Deng, L.; Kim, D.; Huang, C.; Tian, K. Carbon budgets of wetland ecosystems in China. *Glob. Chang. Biol.* **2019**, *25*, 2061–2076. [[CrossRef](#)]
11. Gao, J.; Feng, J.; Zhang, X.; Yu, F.; Xu, X.; Kuzyakov, Y. Drying-rewetting cycles alter carbon and nitrogen mineralization in litter-amended alpine wetland soil. *Catena* **2016**, *145*, 285–290. [[CrossRef](#)]

12. Wang, H.; Li, X.; Xiao, J.; Ma, M.; Tan, J.; Wang, X.; Geng, L. Carbon fluxes across alpine, oasis, and desert ecosystems in northwestern China: The importance of water availability. *Sci. Total Environ.* **2019**, *697*, 133978. [[CrossRef](#)]
13. Kang, X.; Li, Y.; Wang, J.; Yan, L.; Zhang, X.; Wu, H.; Yan, Z.; Zhang, K.; Hao, Y. Precipitation and temperature regulate the carbon allocation process in alpine wetlands: Quantitative simulation. *J. Soil. Sediment.* **2020**, *20*, 3300–3315. [[CrossRef](#)]
14. Zhu, J.; Zhang, F.; Li, H.; He, H.; Li, Y.; Yang, Y.; Zhang, G.; Wang, C.; Luo, F. Seasonal and interannual variations of CO<sub>2</sub> fluxes over 10 years in an alpine wetland on the Qinghai-Tibetan Plateau. *J. Geophys. Res. Biogeosciences* **2020**, *125*, e2020J–e6011J. [[CrossRef](#)]
15. He, G.; Li, K.; Liu, X.; Gong, Y.; Hu, Y. Fluxes of methane, carbon dioxide and nitrous oxide in an alpine wetland and an alpine grassland of the Tianshan Mountains, China. *J. Arid Land* **2014**, *6*, 717–724. [[CrossRef](#)]
16. Heikkinen, J.E.P.; Elsakov, V.; Martikainen, P.J. Carbon dioxide and methane dynamics and annual carbon balance in tundra wetland in NE Europe, Russia. *Glob. Biogeochem. Cycles* **2002**, *16*, 61–62. [[CrossRef](#)]
17. Zhao, L.; Li, J.; Xu, S.; Zhou, H.; Li, Y.; Gu, S.; Zhao, X. Seasonal variations in carbon dioxide exchange in an alpine wetland meadow on the Qinghai-Tibetan Plateau. *Biogeosciences* **2010**, *7*, 1207–1221. [[CrossRef](#)]
18. McFadden, J.P.; Eugster, W.; Chapin, F.S. A regional study of the controls on water vapor and CO<sub>2</sub> exchange in arctic tundra. *Ecology* **2003**, *84*, 2762–2776. [[CrossRef](#)]
19. Kang, X.; Hao, Y.; Cui, X.; Chen, H.; Huang, S.; Du, Y.; Li, W.; Kardol, P.; Xiao, X.; Cui, L. Variability and Changes in Climate, Phenology, and Gross Primary Production of an Alpine Wetland Ecosystem. *Remote Sens.* **2016**, *8*, 391. [[CrossRef](#)]
20. Yuan, X.; Chen, Y.; Qin, W.; Xu, T.; Mao, Y.; Wang, Q.; Chen, K.; Zhu, B. Plant and microbial regulations of soil carbon dynamics under warming in two alpine swamp meadow ecosystems on the Tibetan Plateau. *Sci. Total Environ.* **2021**, *790*, 148072. [[CrossRef](#)]
21. Park, S.; Knohl, A.; Migliavacca, M.; Thum, T.; Vesala, T.; Peltola, O.; Mammarella, I.; Prokushkin, A.; Kolle, O.; Lavrič, J.; et al. Temperature Control of Spring CO<sub>2</sub> Fluxes at a Coniferous Forest and a Peat Bog in Central Siberia. *Atmosphere* **2021**, *12*, 984. [[CrossRef](#)]
22. Bridgman, S.D.; Megonigal, J.P.; Keller, J.K.; Bliss, N.B.; Trettin, C. The carbon balance of North American wetlands. *Wetlands* **2006**, *26*, 889–916. [[CrossRef](#)]
23. Yu, L.; Wang, H.; Wang, Y.; Zhang, Z.; Chen, L.; Liang, N.; He, J. Temporal variation in soil respiration and its sensitivity to temperature along a hydrological gradient in an alpine wetland of the Tibetan Plateau. *Agric. For. Meteorol.* **2020**, *282–283*, 107854. [[CrossRef](#)]
24. Miao, Y.; Liu, M.; Xuan, J.; Xu, W.; Wang, S.; Miao, R.; Wang, D.; Wu, W.; Liu, Y.; Han, S. Effects of warming on soil respiration during the non-growing seasons in a semiarid temperate steppe. *J. Plant Ecol.* **2020**, *13*, 288–294. [[CrossRef](#)]
25. Zhang, F.; Liu, A.; Li, Y.; Zhao, L.; Wang, Q.; Du, M. CO<sub>2</sub> flux in alpine wetland ecosystem on the Qinghai-Tibetan Plateau, China. *Acta Ecol. Sin.* **2008**, *28*, 453–462.
26. Jin, Z.; Zhuang, Q.; He, J.; Zhu, X.; Song, W. Net exchanges of methane and carbon dioxide on the Qinghai-Tibetan Plateau from 1979 to 2100. *Environ. Res. Lett.* **2015**, *10*, 85007. [[CrossRef](#)]
27. Niu, Z.; Zhang, H.; Wang, X.; Yao, W.; Zhou, D.; Zhao, K.; Zhao, H.; Li, N.; Huang, H.; Li, C.; et al. Mapping wetland changes in China between 1978 and 2008. *Chin. Sci. Bull.* **2012**, *57*, 2813–2823. [[CrossRef](#)]
28. Cao, S.; Cao, G.; Chen, K.; Han, G.; Liu, Y.; Yang, Y.; Li, X. Characteristics of CO<sub>2</sub>, water vapor, and energy exchanges at a headwater wetland ecosystem of the Qinghai Lake. *Can. J. Soil Sci.* **2019**, *99*, 227–243. [[CrossRef](#)]
29. Cao, S.; Cao, G.; Feng, Q.; Han, G.; Lin, Y.; Yuan, J.; Wu, F.; Cheng, S. Alpine wetland ecosystem carbon sink and its controls at the Qinghai Lake. *Environ. Earth Sci.* **2017**, *76*, 210. [[CrossRef](#)]
30. Burba, G. *Eddy Covariance Method: For Scientific, Industrial, Agricultural and Regulatory Applications*; LI-COR Biosciences: Lincoln, NE, USA, 2013.
31. Foken, T.; Göckede, M.; Mauder, M.; Mahrt, L.; Amiro, B.; Munger, W. Post-field data quality control. In *Handbook of Micrometeorology*; Lee, X., Massman, W., Law, B., Eds.; Springer: Dordrecht, The Netherlands, 2005; pp. 181–208.
32. Zhang, L.; Luo, Y.; Liu, M.; Chen, Z.; Su, W.; He, H.; Zhu, Z.; Sun, X.; Wang, Y.; Zhou, G.; et al. Carbon and water fluxes observed by the Chinese Flux Observation and Research Network (2003–2005). *Sci. Data Bank* **2019**, *4*, 1–17.
33. Elith, J.; Leathwick, J.R.; Hastie, T. A working guide to boosted regression trees. *J. Anim. Ecol.* **2008**, *77*, 802–813. [[CrossRef](#)]
34. Sun, S.; Che, T.; Li, H.; Wang, T.; Ma, C.; Liu, B.; Wu, Y.; Song, Z. Water and carbon dioxide exchange of an alpine meadow ecosystem in the northeastern Tibetan Plateau is energy-limited. *Agric. For. Meteorol.* **2019**, *275*, 283–295. [[CrossRef](#)]
35. Li, H.; Wang, C.; Zhang, F.; He, Y.; Shi, P.; Guo, X.; Wang, J.; Zhang, L.; Li, Y.; Cao, G.; et al. Atmospheric water vapor and soil moisture jointly determine the spatiotemporal variations of CO<sub>2</sub> fluxes and evapotranspiration across the Qinghai-Tibetan Plateau grasslands. *Sci. Total Environ.* **2021**, *791*, 148379. [[CrossRef](#)] [[PubMed](#)]
36. Zhang, F.; Li, H.; Wang, W.; Li, Y.; Lin, L.; Guo, X.; Du, Y.; Li, Q.; Yang, Y.; Cao, G.; et al. Net radiation rather than moisture supply governs the seasonal variations of evapotranspiration over an alpine meadow on the northeastern Qinghai-Tibetan Plateau. *Ecohydrology* **2018**, *11*, e1925. [[CrossRef](#)]
37. Li, H.; Zhu, J.; Zhang, F.; He, H.; Yang, Y.; Li, Y.; Cao, G.; Zhou, H. Growth stage-dependant variability in water vapor and CO<sub>2</sub> exchanges over a humid alpine shrubland on the northeastern Qinghai-Tibetan Plateau. *Agric. For. Meteorol.* **2019**, *268*, 55–62. [[CrossRef](#)]
38. Lefcheck, J.S. piecewiseSEM: Piecewise structural equation modelling in r for ecology, evolution, and systematics. *Methods Ecol. Evol.* **2016**, *7*, 573–579. [[CrossRef](#)]

39. R Development Core Team. *R: A Language and Environment for Statistical Computing*; R Foundation for Statistical Computing: Vienna, Austria, 2006.
40. Hao, Y.B.; Cui, X.Y.; Wang, Y.F.; Mei, X.R.; Kang, X.M.; Wu, N.; Luo, P.; Zhu, D. Predominance of Precipitation and Temperature Controls on Ecosystem CO<sub>2</sub> Exchange in Zoige Alpine Wetlands of Southwest China. *Wetlands* **2011**, *31*, 413–422. [[CrossRef](#)]
41. Chapin, F.S.; Matson, P.A.; Mooney, H.A. *Principles of Terrestrial Ecosystem Ecology*, 2nd ed.; Springer: New York, NY, USA, 2011.
42. Humphrey, V.; Berg, A.; Ciais, P.; Gentile, P.; Jung, M.; Reichstein, M.; Seneviratne, S.I.; Frankenberg, C. Soil moisture-atmosphere feedback dominates land carbon uptake variability. *Nature* **2021**, *592*, 65–69. [[CrossRef](#)] [[PubMed](#)]
43. Huang, M.; Piao, S.; Ciais, P.; Peñuelas, J.; Wang, X.; Keenan, T.F.; Peng, S.; Berry, J.A.; Wang, K.; Mao, J.; et al. Air temperature optima of vegetation productivity across global biomes. *Nat. Ecol. Evol.* **2019**, *3*, 772–779. [[CrossRef](#)]
44. Körner, C. *Alpine Plant Life: Functional Plant Ecology of High Mountain Ecosystems*, 2nd ed.; Springer: Berlin/Heidelberg, Germany, 2003.
45. Zhang, T.; Zhang, Y.; Xu, M.; Zhu, J.; Chen, N.; Jiang, Y.; Huang, K.; Zu, J.; Liu, Y.; Yu, G. Water availability is more important than temperature in driving the carbon fluxes of an alpine meadow on the Tibetan Plateau. *Agric. For. Meteorol.* **2018**, *256–257*, 22–31. [[CrossRef](#)]
46. Quan, Q.; Tian, D.; Luo, Y.; Zhang, F.; Crowther, T.W.; Zhu, K.; Chen, H.Y.H.; Zhou, Q.; Niu, S. Water scaling of ecosystem carbon cycle feedback to climate warming. *Sci. Adv.* **2019**, *5*, v1131. [[CrossRef](#)] [[PubMed](#)]
47. Ding, J.; Yang, T.; Zhao, Y.; Liu, D.; Wang, X.; Yao, Y.; Peng, S.; Wang, T.; Piao, S. Increasingly Important Role of Atmospheric Aridity on Tibetan Alpine Grasslands. *Geophys. Res. Lett.* **2018**, *45*, 2852–2859. [[CrossRef](#)]
48. Wang, Y.; Wang, H.; He, J.; Feng, X. Iron-mediated soil carbon response to water-table decline in an alpine wetland. *Nat. Commun.* **2017**, *8*, 15972. [[CrossRef](#)] [[PubMed](#)]